ISSN 1024-8560, Atmospheric and Oceanic Optics, 2022, Vol. 35, No. 6, pp. 775–781.

Backscattering Characteristics of Optical and Electromagnetic Waves in Joint Sensing of Cirrus Clouds by a Polarizing Lidar (0.355 μm) and a 94-GHz Radar

V. A. Shishko[a, b, *], D. N. Timofeev[a], A. V. Konoshonkin[a, **], N. V. Kustova[a], N. Kan[a], I. V. Tkachev[a], K. Masuda[c], H. Ishimoto[c], H. Okamoto[d], and A. G. Borovoi[a]

[a] *V.E. Zuev Institute of Atmospheric Optics, Siberian Branch, Russian Academy of Sciences, Tomsk, 634055 Russia*
[b] *National Research Tomsk State University, Tomsk, 634050 Russia*
[c] *Meteorological Research Institute, Nagamine 1-1, Tsukuba 305-0052, Japan*
[d] *Kyushu University, Kasuga, Fukuoka 816-8580, Japan*
**e-mail: sva@iao.ru*
***e-mail: sasha_tvo@iao.ru*

Received April 8, 2022; revised May 13, 2022; accepted June 15, 2022

Abstract—In this work, the problem of radiation scattering by ice crystals typical for cirrus clouds is solved for a 94-GHz radar (wavelength 3189 μm) and a lidar (wavelength 0.355 μm); the ice refractive indices are $1.7864 + 0.0032i$ and $1.3249 + 0i$, respectively. The scattering matrices are calculated within the physical optics approximation and the discrete dipole approximation for the case of randomly oriented particles with sizes from 4 to 1000 μm. The ratio of the radar and lidar backscattering signals in the backward direction (the so-called radar–lidar ratio) is calculated for a wide range of the particle size for typical shapes of cirrus cloud ice crystals. It is shown that this ratio can be used for estimating the size of ice crystals in cirrus clouds.

Keywords: light scattering, lidar, radar, physical optics, discrete dipole approximation, atmospheric ice crystals, cirrus clouds

DOI: 10.1134/S1024856022060239

INTRODUCTION

The global climatic changes observed in recent time require a closer and more detailed study of climate-forming factors [1, 2]. One of main sources of uncertainty in present-day numerical models of climate change forecasting is cirrus clouds, which are an important atmospheric component having a significant effect on the radiation budget of the Earth [3–8]. Cirrus clouds are usually located at altitudes from 7 to 12 km and consist of mostly hexagonal crystalline ice particles [9, 10].

Microphysical properties (size, shape, orientation, etc.) of atmospheric ice crystals are poorly studied due to the high degree of their variability in time and space, as well as by virtue of the fact that field measurements of such properties are ineffective due to the break of the particle structure at the instant of observations [11, 12]. Various remote methods remain effective ways of studying the atmosphere. Among them, methods of lidar and radar sensing stand out. They provide active cloud sensing [13–19] with the use of ground-based, airborne, and spaceborne devices [13, 19–23]. The advantage of these methods is that they make no changes in the spatial orientation of crystals. However, there appear difficulties in interpreting signals received in these methods [24–26].

Earlier [27, 28], we found lidar-measured characteristics (the lidar, depolarization, and spectral ratios) that are sensitive to the shape and orientation of atmospheric ice crystals. It was proposed to use these characteristics for classification of ice particle types as applied to operation of the ATLID (ATmospheric LIDar) high spectral resolution lidar [29, 30]. The problem of determining the size of ice crystals remains unsolved because there are as yet no effective algorithms for retrieving the size of cirrus cloud ice particles and the data obtained by laser sensing of the atmosphere weakly depend on the particle size [28].

Information about the size of atmospheric ice crystals is necessary for solving such climatic problems as the problem of radiation transfer, prediction of global disasters, and others, as well as for inclusion into present-day models of the global climate change and long-term weather forecasts.

The idea of joint sensing the same volume of a cirrus cloud by a lidar and a radar seems to be promising for solving the problem of determining the size of cloud crystals under the assumption that the distribu-

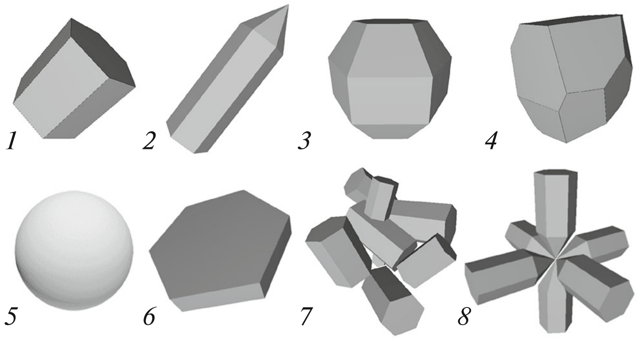

Fig. 1. Ice crystal shapes used in the calculations: (*1*) hexagonal column; (*2*) bullet; (*3*) droxtal; (*4*) arbitrary shape; (*5*) sphere; (*6*) hexagonal plate; (*7*) aggregate; and (*8*) bullet-rosette.

tions of ice crystals and their microphysical characteristics during such measurements remain unchanged.

As we have already shown in [31], the ratio of radar to lidar backscattering signals (the radar–lidar ratio) in the process of joint sensing the same volume of a cirrus cloud by a lidar and a radar does not depend on the specific number of particles and, as a consequence, characterizes only microphysics of ice crystals. This is caused by the fact that the radar signal is mainly determined by the specific volume of the particles under study and the lidar signal is mainly sensitive to the particle projection area. As a consequence, their ratio is sensitive just to the particle size.

In spite of the absence of the theoretical solution, experiments on joint sensing of the cirrus cloudiness by a lidar and a radar have been carried out for about 30 years. The first work combining lidar and radar measurements of cirrus clouds was performed in 1993 by Intrieri et al. [32]. The authors could retrieve the vertical profiles of the effective size of a crystal from data of joint measurements by a lidar and a radar. However, because of insufficient development of numerical methods in 1993, scattering by cirrus cloud particles was modeled within the framework of the Lorentz–Mie theory [33, 34], which is not correct because the shape and orientation of nonspherical particles mostly observed in cirrus clouds [12, 35] have a significant effect on light scattering [36]. In spite of this shortcoming, the work became widely known and its results are used for interpreting experimental data [18, 37–40]. However, the problem of accuracy in retrieving the average size of cirrus cloud ice particles when using the above suggested technique remains unsolved. Later, other algorithms of joint simultaneous measurements by space radiometers, radars, and lidars were developed and studied (for example, [18, 37–40]). We also corroborated the possibility and effectiveness of retrieving particle size from data of joint sensing in theoretical calculations for a 35-GHz radar (the wavelength $\lambda = 8565$ μm) and a lidar (0.532 μm) mounted in southeast China (Anhui Institute of Optics and Fine Mechanics, Hefei) [31].

As soon as in March 2023, the EarthCARE (Earth Clouds, Aerosols and Radiation Explorer) satellite [41], on board of which the ATLID lidar ($\lambda = 0.355$ μm) and the CPR (Cloud Profiling Radar) radar at a frequency of 94 GHz ($\lambda = 3189$ μm) are to jointly operate, will be launched into Earth orbit. In connection with this, it is necessary to construct an optical model of cirrus cloudiness for the wavelengths of the ATLID lidar CPR radar mounted on the satellite with the aim of interpreting the data of joint sensing by the lidar and radar. This work is devoted to solving this problem.

METHODOLOGY

To construct the optical model of cirrus clouds for wavelengths of the ATLID lidar and CPR radar mounted on the *EarthCARE* satellite, the database necessary for interpreting the joint measurements by the radar and lidar was calculated on the computational cluster of the Institute of Atmospheric Optics, Siberian Branch, Russian Academy of Sciences. Instead of the quantities measured experimentally, the theoretical calculations involve light backscattering matrices $\mathbf{M}^{\mathrm{lid}}$ (the Mueller matrix [42]) for the lidar wavelengths and backscattering matrices of microwave radiation $\mathbf{M}^{\mathrm{rad}}$ for the radar wavelengths.

For the ATLID lidar ($\lambda = 0.355$ μm), the light backscattering matrices for spherical particles were calculated within the framework of the Lorentz–Mie theory [34, 43]; for all other types of particles, the physical optics method [44, 45] was used. The refractive index of ice was taken as 1.3249 + 0*i*. For the 94-GHz CPR radar ($\lambda = 3189$ μm), the backscattering matrices of microwave radiation were calculated in the discrete dipole approximation developed by Yurkin [46, 47]; in that case, the refractive index of ice was taken as 1.7864 + 0.0032*i*.

The following shapes of randomly oriented particles were simulated: hexagonal columns and plates, bullets, droxtals, aggregates, bullet-rosettes, particles of an arbitrary shape, and spherical particles (Fig. 1). When simulating by the discrete dipole method, the particles were represented by a set of 4000 to 20000 dipoles depending on the particle size.

It is accepted to define dimensions of large nonspherical cirrus cloud particles by their maximal size (the distance between the most remote points of the particle) $D_{\max}$ [48]; in our calculations, it varied within the range from 4 to 1000 μm. Thus, the typical crystal size significantly exceeds the wavelength of the lidar but is less than the wavelength of the radar.

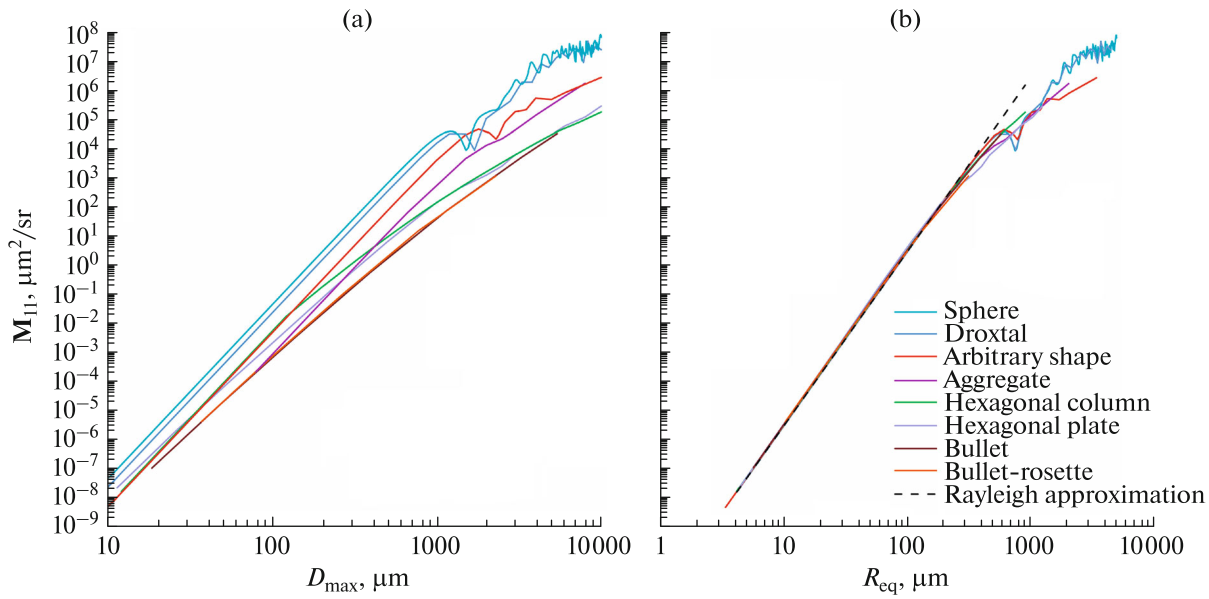

Fig. 2. Element of the backscattering matrix of microwave radiation $\mathbf{M}_{11}^{rad}$ for randomly oriented crystals with different shapes as a function of (a) the maximal particle size D_{max} and (b) the equivalent radius R_{eq}. The CPR wavelength is 3189 μm.

RESULTS

When solving the problem of light scattering by particles much smaller than the incident radiation wavelength, the solution can be analytically represented; this is the so-called Rayleigh scattering (Rayleigh approximation) [49]. However, calculations obtained by the discrete dipole method demonstrate that the Rayleigh approximation is inapplicable to particles with a size exceeding 200 μm for the radar wavelength 3189 μm. Figure 2a shows the element $\mathbf{M}_{11}^{rad}$ of the scattering matrix as a function of D_{max}. It is seen that the solution has a strong scatter depending on the particle shape. This contradiction can be explained with allowance for the fact that scattering by particles much smaller than the incident radiation wavelength depends not on the size but on the volume of a particle. For this reason, we propose to introduce another parameter characterizing the particle size, namely, the equivalent radius R_{eq} which has a simple physical meaning: this is the radius of a sphere whose volume coincides with the volume of the particle under study:

$$R_{eq} = \sqrt[3]{\frac{3V_{part}}{4\pi}},$$

where V_{part} is the volume of the nonspherical particle.

Comparison of Figs. 2a and 2b shows that the definition of the particle size via the equivalent radius R_{eq} instead of the commonly accepted maximal size D_{max} allows one to obtain a good agreement with the Rayleigh approximation for all types of particles in the size range $R_{eq} < 200$ μm for the 94-Ghz radar.

We have already obtained the solution of the problem of light scattering for the ATLID lidar with $\lambda = 0.355$ μm [28] and presented it in the database [50]. As an illustration, Fig. 3 shows the element $\mathbf{M}_{11}^{lid}$ of the light backscattering matrix as a function of the maximal size D_{max} and equivalent radius R_{eq} of the particle.

After we could solve the problem of scattering by cirrus cloud ice particles as applied to the ATLID and CPR, we could calculate the radar–lidar ratio.

Figure 4 shows the radar–lidar ratio calculated by the formula

$$\chi = \frac{\beta^r}{\beta^l} = \frac{c\sigma^r}{c\sigma^l} = \frac{\sigma^r}{\sigma^l} = \frac{\mathbf{M}_{11}^{rad}}{\mathbf{M}_{11}^{lid}}. \quad (1)$$

Here, $\beta^{r,l}$ is the backscattering coefficient of the radar and lidar radiation; c is the particle density in the cloud; $\sigma^{r,l}$ is the differential back scattering cross section of a single crystal (it is averaged over the statistical ensemble of crystals in the cloud); and $\mathbf{M}_{11}^{lid}$ and $\mathbf{M}_{11}^{rad}$ were obtained when the scattering problem was solved by the physical optics method and in the discrete dipole approximation, respectively. The solution was obtained for ice particles presented in Fig. 1 as a function of the crystal maximal size (Fig. 4a) and the equivalent radius (Fig. 4b). Here, we assume the particle density to be equal in the cloud regions distinguished by the lidar and the radar is the same.

It is seen from Fig. 4 that the definition of the particle size in terms of the equivalent radius R_{eq} is preferable when using the ratio χ for retrieving the size because the curves, obviously, weakly depend on crystal shapes and

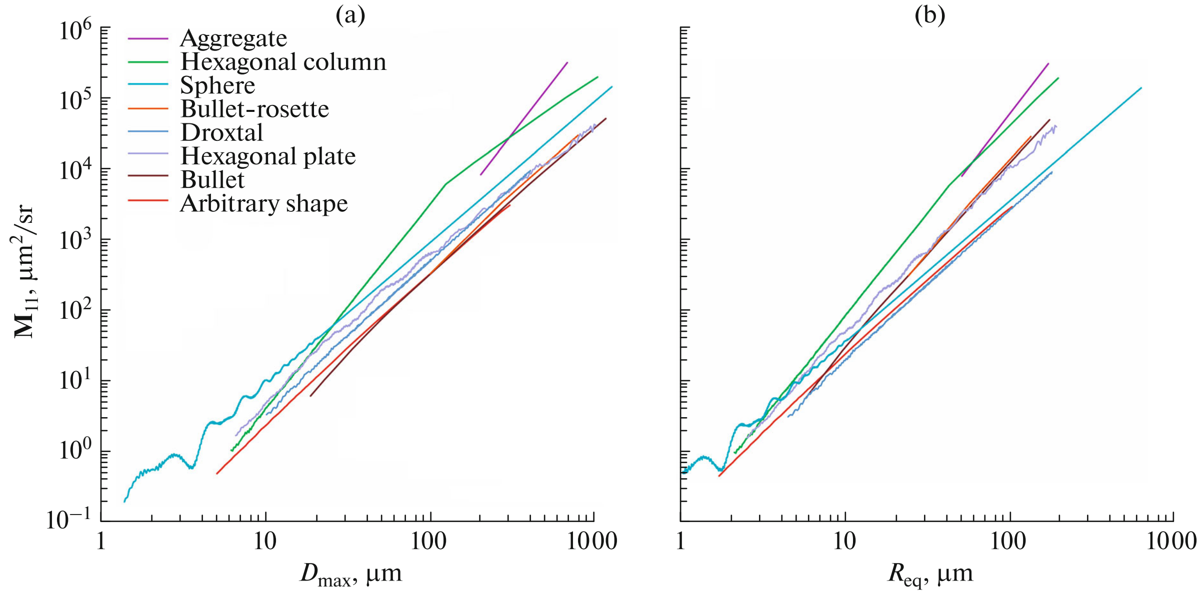

Fig. 3. Element of the light backscattering matrix $\mathbf{M}_{11}^{lid}$ for randomly oriented crystals with different shapes as a function of (a) the maximum particle size D_{max} and (b) the equivalent radius R_{eq}. The ATLID wavelength is 0.355 μm.

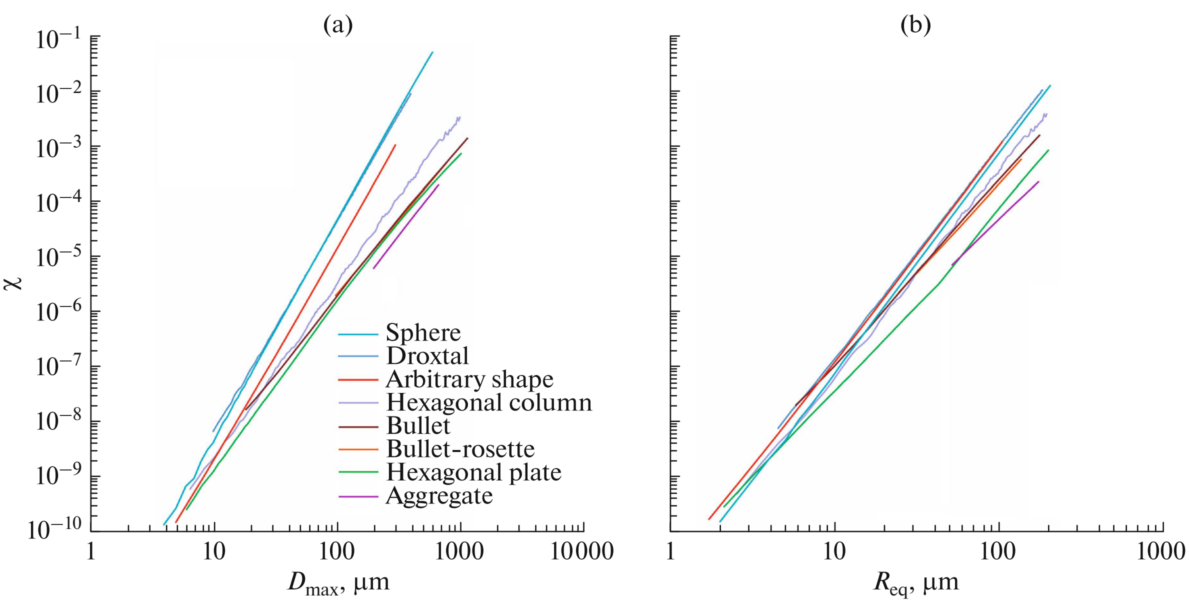

Fig. 4. Radar–lidar ratio for randomly oriented crystals with different shapes as a function of (a) the maximum particle size and (b) the equivalent radius. The wavelengths of the lidar and radar (94 GHz) 0.355 and 3189 μm, respectively.

the dependence on the crystal size remains strong. These results corroborate that the radar–lidar ratio is effective for retrieving the crystal size.

DISCUSSION

Formula (1) involves the following assumptions: a radar and a lidar observe the same ensemble of ice crystals (although the fields of vision of the instruments are different) and the cloud is homogeneous both in the orientation of the crystals and in their size. Within the scope of this work, we do not consider the question of how such assumptions are allowable; therefore, special attention should be paid to this when interpreting the experimental data. Besides, ice crystals in cirrus clouds are not monodisperse but are distributed over sizes. Since the question of choosing the law of crystal size distribution is still under discussion,

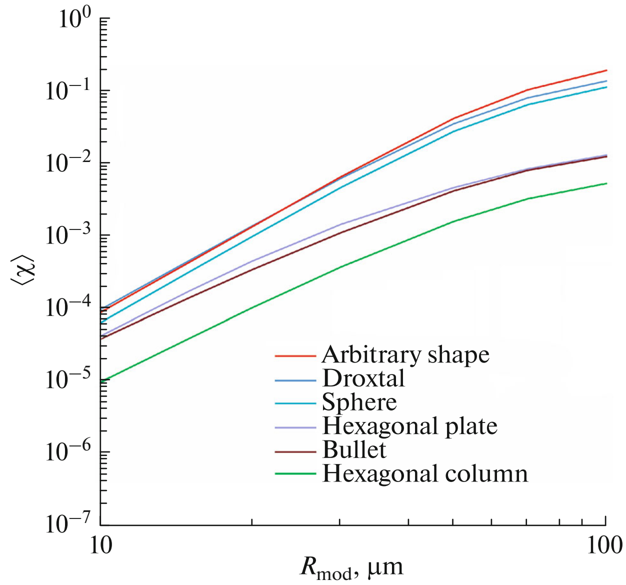

Fig. 5. Radar–lidar ratio for randomly oriented crystals with different shapes as a function of the modal radius. The wavelengths of the lidar and radar (94 GHz) are 0.355 and 3189 μm, respectively.

we chose the gamma distribution proposed in works by Okamoto [51, 52] as a preliminary estimate.

Let us estimate the effect of the size distribution on the radar–lidar ratio using the gamma distribution in its simplest form ($k = 2$):

$$p(R_{eq}) = R_{eq}^{k-1}\frac{\exp(-R_{eq}/\theta)}{\theta^k\Gamma(k)},$$

where p is the probability density; $\Gamma(k)$ is the gamma function; and θ and k are the parameters of the gamma distribution.

The radar–lidar ratios averaged with the use of the gamma distribution over the ensemble of ice crystals with a fixed shape are shown in Fig. 5 as functions of the modal radius $R_{mod} = (k - 1)\theta$ which has a simple physical meaning: this is the most frequent crystal size in the distribution.

As seen from Fig. 5, ensemble averaging of particles in the cloud has an effect on the absolute value of the radar–lidar ratio χ; however, the dependence on size still remains strong. It is seen that a change in the modal size by an order of magnitude (from 10 to 100 μm) leads to a change in χ almost by three orders. This fact proves the effectiveness of using the radar–lidar ratio for determining the particle size in a cloud.

Certainly, the proposed law of the particle size gamma distribution is of illustrative character and the problem of choosing an adequate particle size distribution in a cloud should be considered in detail later.

CONCLUSIONS

Thus, within the framework of the physical optics approximation and discrete dipole method, the ratio of the radar signal to the lidar signal has been calculated for the first time for a realistic model of dimensions and shapes of cirrus cloud ice crystals for the *EarthCARE* spacecraft. It has been shown that it is the radar–lidar ratio that is the most informative for reconstructing the size of crystals regardless of their shape. It is planned to use the results obtained when creating algorithms for interpreting data of joint sensing by the lidar and the radar of the *EarthCARE* satellite.

FUNDING

The calculations were supported by the Russian Science Foundation (project no. 21-77-00083).

CONFLICT OF INTEREST

The authors declare that they have no conflicts of interest.

OPEN ACCESS

REFERENCES

1. B. M. Baker, "Cloud microphysics and climate," Science **276**, 1072–1078 (1997).
2. *Climate Change 2007: The Physical Science Basis. Contribution of Working Group I to the Fourth Assessment Report of the Intergovernmental Panel on Climate Change,* Ed. by S. Solomon, D. Qin, M. Manning, Z. Chen, M. Marquis, K.B. Averyt, M. Tignor, and H.L. Miller (Cambridge University Press, Cambridge, New York, 2007).
3. P. Wendling, R. Wendling, and H. K. Weickmann, "Scattering of solar radiation by hexagonal ice crystals," Appl. Opt. **18**, 2663–2671 (1979).
4. K. N. Liou, "Influence of cirrus clouds on weather and climate processes: A global perspective," Mon. Weather Rev. **114** (6), 1167–1199 (1986).
5. Y. Takano and K. N. Liou, "Radiative transfer in cirrus clouds. Part III: Light scattering by irregular ice crystals," J. Atmos. Sci. **52** (7), 818–837 (1995).

6. K. Sassen and S. Benson, "A midlatitude cirrus cloud climatology from the facility for atmospheric remote sensing: II. Microphysical properties derived from lidar depolarization," J. Atmos. Sci. **58** (15), 2103–2112 (2001).

7. K. Sassen, J. Zhu, and S. Benson, "Midlatitude cirrus cloud climatology from the facility for atmospheric remote sensing. IV. Optical displays," Appl. Opt. **42**, 332–341 (2003).

8. Y. Takano and K. N. Liou, "Solar radiative transfer in cirrus clouds. Part I. Single scattering and optical properties of hexagonal ice crystals," J. Atmos. Sci. **46** (1), 3–19 (1989).

9. P. V. Hobbs, S. Chang, and J. D. Locatelli, "The dimensions and aggregation of ice crystals in natural clouds," J. Geophys. Res. **79**, 2199–2206 (1974).

10. J. Um and G. M. McFarquhar, "Formation of atmospheric halos and applicability of geometric optics for calculating single-scattering properties of hexagonal ice crystals: Impacts of aspect ratio and ice crystal size," J. Quant. Spectrosc. Radiat. Transfer **165**, 134–152 (2015).

11. B. A. Baker and R. P. Lawson, "In situ observations of the microphysical properties of wave, cirrus, and anvil clouds. Part I: Wave clouds," J. Atmos. Sci. **63**, 3160–3185 (2006).

12. J. Um, G. M. McFarquhar, Y. P. Hong, S.-S. Lee, C. H. Jung, R. P. Lawson, and Q. Mo, "Dimensions and aspect ratios of natural ice crystals," Atmos. Chem. Phys. **15**, 3933–3956 (2015).

13. F. Moshary, Z. Han, Y. Wu, B. Gross, D. Wesloh, R. M. Hoff, R. Delgado, J. Su, L. Lei, R. B. Lee, M. P. McCormick, J. Diaz, C. Cruz, and H. Parsiani, "New results from the NOAA CREST lidar network (CLN) observations in the US Eastcoast," EPJ Web of Conf. **119**, 19005 (2016).

14. I. Veselovskii, P. Goloub, T. Podvin, D. Tanre, A. Ansmann, M. Korenskiy, A. Borovoi, Q. Hu, and D. N. Whiteman, "Spectral dependence of backscattering coefficient of mixed phase clouds over west Africa measured with two-wavelength Raman POLARIZATION Lidar: Features attributed to ice-crystals corner reflection," J. Quant. Spectrosc. Radiat. Transfer **202**, 74–80 (2017).

15. Y. S. Balin, S. V. Samoilova, M. M. Krekova, and D. M. Winker, "Retrieval of cloud optical parameters from space-based backscatter lidar data," Appl. Opt. **38** (30), 6365–6373 (1999).

16. G. P. Kokhanenko, Yu. S. Balin, M. G. Klemasheva, S. V. Nasonov, M. M. Novoselov, I. E. Penner, and S. V. Samoilova, "Scanning polarization lidar LOSA-M3: Opportunity for research of crystalline particle orientation in the clouds of upper layers," Atmos. Meas. Tech. **13** (3), 1113–1127 (2020).

17. H. Okamoto, A. Macke, M. Quante, and E. Raschke, "Modeling of backscattering by nonspherical ice particles for the interpretation of cloud radar signals at 94 GHz. An error analysis," Beitr. Phys. Atmos. **68**, 319–334 (1995).

18. C.-L. Liu and A. J. Illingworth, "Toward more accurate retrievals of ice water content from radar measurements of clouds," J. Appl. Meteorol. **39** (7), 1130–1146 (2000).

19. A. Zabukovec, G. Ancellet, I. E. Penner, M. Arshinov, V. Kozlov, J. Pelon, J.-D. Paris, G. Kokhanenko, Y. S. Balin, D. Chernov, and B. D. Belan, "Characterization of aerosol sources and optical properties in Siberia using airborne and spaceborne observations," Atmosphere **12** (2) (2021).

20. D. M. Winker, R. H. Couch, and M. P. McCormick, "An overview of LITE: NASA'S lidar-in-space technology experiment," Proc. IEEE **84**, 164–180 (1996).

21. D. M. Winker, J. Pelon, and M. P. McCormick, "The CALIPSO mission: Spaceborne lidar for observation of aerosols and clouds," Proc. SPIE—Int. Soc. Opt. Eng. **4893** (2002).

22. Yu. S. Balin and A. A. Tikhomirov, "The history of development and operaion of the first Russian space lidar BALKAN integrated into Mir space station," Opt. Atmos. Okeana **24** (12), 1078–1087 (2011).

23. K. Sassen, Z. Wang, and D. Liu, "Global distribution of cirrus clouds from CloudSat/Cloud-Aerosol Lidar and Infrared Pathfinder Satellite Observations (CALIPSO) measurements," J. Geophys. Res. **113**, D00A12 (2008).

24. K. J. Garrett, P. Yang, S. L. Nasiri, C. R. Yost, and B. A. Baum, "Influence of cloud top height and geometric thickness on MODIS infrared-based cirrus cloud retrieval," J. Appl. Meteorol. Climatol. **48**, 818–832 (2009).

25. V. A. Shishko, I. D. Bryukhanov, E. V. Nie, N. V. Kustova, D. N. Timofeev, and A. V. Konoshonkin, "Algorithm for interpreting light backscattering matrices of cirrus clouds for the retrieval of their microphysical parameters," Atmos. Ocean. Opt. **32** (4), 393–399 (2019).

26. H. Okamoto, S. Iwasaki, M. Yasui, H. Horie, H. Kuroiwa, and H. Kumagai, "An algorithm for retrieval of cloud microphysics using 95-GHz cloud radar and lidar," J. Geophys. Res. **108** (D7), 4226 (2003).

27. A. Borovoi, A. Konoshonkin, N. Kustova, and H. Okamoto, "Backscattering Mueller matrix for quasihorizontally oriented ice plates of cirrus clouds: Application to CALIPSO signals," Opt. Express **20**, 28222–28233 (2012).

28. A. Konoshonkin, A. Borovoi, N. Kustova, and J. Reichardt, "Power laws for backscattering by ice crystals of cirrus clouds," Opt. Express **25** (19), 22341–22346 (2017).

29. H. Okamoto, K. Sato, A. Borovoi, H. Ishimoto, K. Masuda, A. Konoshonkin, and N. Kustova, "Interpretation of lidar ratio and depolarization ratio of ice clouds using spaceborne high-spectral-resolution polarization lidar," Opt. Express **27** (25), 36587–36600 (2019).

30. H. Okamoto, K. Sato, A. Borovoi, H. Ishimoto, K. Masuda, A. Konoshonkin, and N. Kustova, "Wavelength dependence of ice cloud backscatter properties for space-borne polarization lidar applications," Opt. Express **28** (20), 29178–29191 (2020).

31. Z. Wang, V. Shishko, N. Kustova, A. Konoshonkin, D. Timofeev, C. Xie, D. Liu, and A. Borovoi, "Radar-lidar ratio for ice crystals of cirrus clouds," Opt. Express **29** (3), 4464–4474 (2021).

32. J. M. Intrieri, G. L. Stephens, W. L. Eberhard, and T. Uttal, "A method for determining cirrus cloud parti-

cle sizes using lidar and radar backscatter technique," J. Appl. Meteorol. **32**, 1074–1082 (1993).

33. G. Mie, "Beitrage Zur Optik Truber Medien, Speziell Kolloidaler Metallosungen," Ann. Phys. (New York) **25**, 377–445 (1908).
34. W. J. Wiscombe, "Improved Mie scattering algorithms," Appl. Opt. **19**, 1505–1509 (1980).
35. A. J. Heymsfield, "Ice crystal terminal velocities," J. Atmos. Sci. **29**, 1348–1357 (1972).
36. Yu. S. Balin, B. V. Kaul', and G. P. Kokhanenko, "Observations of specularly reflective particles and layers in crystal clouds," Opt. Atmos. Okeana **25** (4), 293–299 (2011).
37. L. A. Borg, R. E. Holz, and D. D. Turner, "Investigating cloud radar sensitivity to optically thin cirrus using collocated Raman lidar observations," Geophys. Rev. Lett. **38** (2011).
38. C. Tinel, J. Testud, J. Pelon, R. J. Hogan, A. Protat, J. Delanoe, and D. Bouniol, "The retrieval of ice-cloud properties from cloud radar and lidar synergy," J. Appl. Meteorol. **44**, 860–875 (2005).
39. J. Delanoe and R. J. Hogan, "Combined CloudSat-CALIPSO-MODIS retrievals of the properties of ice clouds," J. Geophys. Res. **115** (2010). https://doi.org/10.1029/2009JD012346
40. A. Protat, J. Delanoe, E. J. O'Connor, and T. S. L'Ecuer, "The evaluation of CloudSat and CALIPSO ice microphysical products using ground-based cloud radar and lidar observations," J. Atmos. Ocean. Technol **27**, 793–810 (2010).
41. A. J. Illingworth, H. W. Barker, A. Beljaars, M. Ceccaldi, H. Chepfer, N. Clerbaux, J. Cole, J. Delanoe, C. Domenech, D. P. Donovan, S. Fukuda, M. Hirakata, R. J. Hogan, A. Huenerbein, P. Kollias, T. Kubota, T. Nakajima, T. Y. Nakajima, T. Nishizawa, Y. Ohno, H. Okamoto, R. Oki, K. Sato, M. Satoh, M. W. Shephard, A. Velazquez-Blazquez, U. Wandinger, T. Wehr, and G.-J. van Zadelhoff, "The EarthCARE satellite: The next step forward in global measurements of clouds, aerosols, precipitation, and radiation," Bull. Am. Meteorol. Soc. **96** (8), 1311–1332 (2015).
42. M. Hayman and J. P. Thayer, "General description of polarization in lidar using stokes vectors and polar decomposition of Mueller matrices," J. Opt. Soc. Am. A **29**, 400–409 (2012).
43. V. A. Shishko, A. V. Konoshonkin, N. V. Kustova, and D. N. Timofeev, "Light scattering by spherical particles for data interpretation of mobile lidars," Opt. Eng. **59** (8), 083103 (2020).
44. V. A. Shishko, A. V. Konoshonkin, N. V. Kustova, D. N. Timofeev, and A. G. Borovoi, "Coherent and incoherent backscattering by a single large particle of irregular shape," Opt. Express **27** (23), 32984–32993 (2019).
45. D. N. Timofeev, A. V. Konoshonkin, N. V. Kustova, V. A. Shishko, and A. G. Borovoi, "Estimation of the absorption effect on light scattering by atmospheric ice crystals for wavelengths typical for problems of laser sounding of the atmosphere," Atmos. Ocean. Opt. **32** (5), 564–568 (2019).
46. A. Penttila, E. Zubko, K. Lumme, K. Muinonen, M. A. Yurkin, B. Draine, J. Rahola, A. G. Hoekstra, and Yu. Shkuratov, "Comparison between discrete dipole implementations and exact techniques," J. Quant. Spectrosc. Radiat. Transfer **106**, 417–436 (2007).
47. M. A. Yurkin and A. G. Hoekstra, "The discrete-dipole-approximation code ADDA: Capabilities and known limitations," J. Quant. Spectrosc. Radiat. Transfer **112**, 2234–2247 (2011).
48. P. Yang and K. N. Liou, "Light scattering and absorption by nonspherical ice crystals," in *Light Scattering Reviews*, Vol. 1, Ed. By A.A. Kokhanovsky (Springer-Praxis, Chichester, 2006).
49. L. D. Landau and E. M. Lifshits, "Rayleigh scattering in gases and liquids," in *Theoretical Physics. Electrodynamics of Solid Media* (Nauka, Moscow, 1982), vol. VIII, pp. 582–583 [in Russian].
50. ftp://ftp.iao.ru/pub/GWDT/Physical_optics/Backscattering/. Cited April 4, 2022.
51. A. Borovoi, A. Konoshonkin, N. Kustova, and H. Okamoto, "Backscattering Mueller matrix for quasihorizontally oriented ice plates of cirrus clouds: Application to CALIPSO signals," Opt. Express **20**, 28222–28233 (2012).
52. H. Okamoto, K. Sato, and Y. Hagihara, "Global analysis of ice microphysics from CloudSat and CALIPSO: Incorporation of specular reflection in lidar signals," J. Geophys. Res. **115**, D22209 (2010).

Translated by A. Nikol'skii